

REVIEW

Optical coherence tomography in detection of dysplasia and cancer of the gastrointestinal tract and bilio-pancreatic ductal system

Pier Alberto Testoni, Benedetto Mangiavillano

Pier Alberto Testoni, Benedetto Mangiavillano, Division of Gastroenterology and Gastrointestinal Endoscopy, Vita-Salute San Raffaele University, Scientific Institute San Raffaele Hospital, Milan 20132, Italy

Author contributions: Testoni PA designed the research; Mangiavillano B performed the research.

Correspondence to: Pier Alberto Testoni, MD, Division of Gastroenterology & Gastrointestinal Endoscopy, Vita-Salute San Raffaele University, Scientific Institute San Raffaele, Via Olgettina 60, Milan 20132, Italy. testoni.pieralberto@hsr.it

Telephone: +39-2-26432756 Fax: +39-2-26433491

Received: April 14, 2008 Revised: June 16, 2008

Accepted: June 23, 2008

Published online: November 14, 2008

Abstract

Optical coherence tomography (OCT) is an optical imaging modality that performs high-resolution, cross-sectional, subsurface tomographic imaging of the microstructure of tissues. The physical principle of OCT is similar to that of B-mode ultrasound imaging, except that it uses infrared light waves rather than acoustic waves. The *in vivo* resolution is 10-25 times better (about 10 μm) than with high-frequency ultrasound imaging, but the depth of penetration is limited to 1-3 mm, depending upon tissue structure, depth of focus of the probe used, and pressure applied to the tissue surface. In the last decade, OCT technology has evolved from an experimental laboratory tool to a new diagnostic imaging modality with a wide spectrum of clinical applications in medical practice, including the gastrointestinal (GI) tract and pancreatico-biliary ductal system. OCT imaging from the GI tract can be done in humans by using narrow-diameter, catheter-based probes that can be inserted through the accessory channel of either a conventional front-view endoscope, for investigating the epithelial structure of the GI tract, or a side-view endoscope, inside a standard transparent ERCP catheter, for investigating the pancreatico-biliary ductal system. Esophagus and the esophago-gastric junction has been the most widely investigated organ so far; more recently, also duodenum, colon and pancreatico-biliary ductal system have been extensively investigated. OCT imaging of the gastrointestinal wall structure is characterized by a multiple-layer architecture that permits an accurate evaluation of the mucosa, lamina propria, muscularis mucosae, and

part of the submucosa. The technique may be, therefore, used to identify pre-neoplastic conditions of the GI tract, such as Barrett's epithelium and dysplasia, and evaluate the depth of penetration of early-stage neoplastic lesions. OCT imaging of the pancreatic and biliary ductal system could improve the diagnostic accuracy for ductal epithelial changes and the differential diagnosis between neoplastic and non-neoplastic lesions.

© 2008 The WJG Press. All rights reserved.

Key words: Optical coherence tomography; Barrett's epithelium; Dysplasia; Adenocarcinoma; Gastrointestinal tract; Pancreatico-biliary ductal system

Peer reviewer: Aydin Karabacakoglu, PhD, Assistant Professor, Department of Radiology, Meram Medical Faculty, Selcuk University, Konya 42080, Turkey

Testoni PA, Mangiavillano B. Optical coherence tomography in detection of dysplasia and cancer of the gastrointestinal tract and bilio-pancreatic ductal system. *World J Gastroenterol* 2008; 14(42): 6444-6452 Available from: URL: <http://www.wjgnet.com/1007-9327/14/6444.asp> DOI: <http://dx.doi.org/10.3748/wjg.14.6444>

INTRODUCTION

Optical coherence tomography (OCT) is an optical imaging modality, introduced in 1991^[1], that performs high-resolution, cross-sectional, subsurface tomographic imaging of the microstructure in materials and biologic systems by measuring backscattered or backreflected infrared light.

The physical principle of OCT is similar to that of B-mode ultrasound imaging, except that the intensity of infrared light, rather than sound waves, is measured. OCT devices use a low-power infrared light with a wavelength ranging from 750 to 1300 nm in which the only limiting factor is the scattering of light. Scattering occurs when the light interacts with tissue surface and the image formation depends upon the difference in optical backscattering properties of the tissue. OCT images are generated from measuring the echo time delay and the intensity of back-scattered light^[2,3]. Wavelengths of

the infrared light used in OCT are one to two orders of magnitude higher than ultrasound wavelength, so OCT technology can yield a lateral and axial spatial resolution of about 10 μm , which is 10 to 25 fold better than that of available high-frequency ultrasound imaging^[4]. The spatial resolution of OCT images is nearly equivalent to that of histologic sections. The depth of penetration of OCT imaging is approximately 1-3 mm, depending upon tissue structure, depth of focus of the probe used, and pressure applied to the tissue surface. Although the progressive increase in ultrasound resolution is accompanied by a corresponding decrease in depth of penetration, a similar trade-off between resolution and depth of penetration does not occur in OCT imaging.

In OCT, two-dimensional cross-sectional images of tissue microstructure are constructed by scanning the optical beam and performing multiple axial measurements of backscattered light at different transverse positions. The resulting data set is a two-dimensional array that represents the displayed as a grey-scale or false-color image.

Three types of scanning patterns are available for OCT imaging: radial^[5,6], longitudinal^[7,8], and transverse^[9]. The radial-scan probe directs the OCT beam radially, giving images that are displayed in a “radar-like”, circular plot. Radial scanning can easily image large areas of tissue by moving the probe back over the tissue surface and has the highest definition when the probe is inserted within a small diameter lumen, because the OCT images become progressively coarser when a large-diameter lumen is scanned, due to the progressive increase of pixel spacing with increasing the distance between the probe and the tissue. The linear and transverse probes scan the longitudinal and transverse positions of the OCT beam at a fixed angle, generating rectangular images of longitudinal and transverse planes at a given angle with respect to the probe. Linear scanning has the advantage that pixel spacing in the transverse direction is uniform and can better image a definite area of the scanned tissue, especially in presence of large-diameter and non-circular lumens, where maintaining constant distance from the probe to the surface over the entire circumferential scan may be impossible. Transverse scanning modality provides a better depth of field. Depth of field is the range of distances from the probe over which optimal resolution of scanning can be obtained; current OCT scans permit imaging depths of up to 2-3 mm in tissues, by using probes with different focuses.

In the last decade, OCT technology has evolved from an experimental laboratory tool to a new diagnostic imaging modality with a wide spectrum of clinical applications in medical practice, including the gastrointestinal (GI) tract and pancreatico-biliary ductal system.

OCT TECHNIQUE FOR GI TRACT AND PANCREATICO-BILIARY DUCTAL SYSTEM IMAGING

OCT imaging from the GI tract can be done in humans

by using narrow-diameter, catheter-based probes. The probe can be inserted through the accessory channel of either a conventional front-view endoscope, for investigating the epithelial structure of the GI tract, or a side-view endoscope, inside a standard transparent ERCP catheter, for investigating the pancreatico-biliary ductal system.

OCT scanning can be done by maintaining the probe placed lightly or firmly on the wall of the GI tract. When the probe is placed lightly on the mucosal surface, the depth of penetration is limited mainly to the superficial submucosa; by this way superficial epithelium, lamina propria, and the upper part of submucosa are clearly visualized. When the probe is placed firmly against the mucosal surface, submucosa and muscularis propria can be clearly visualized, but details of the superficial layers of the mucosa are lost. When the OCT probe is held in strict contact with the tissue surface, as occurs when it is inserted across strictures of the pancreatico-biliary ductal system, the superficial epithelium may appear compressed and difficult to evaluate.

Several *in vitro* studies demonstrated the feasibility of OCT in the GI tract: In these studies the GI tract wall was identified as a multiple layer structure characterized by a sequence of hyper- and hypo-reflective layers, with a variable homogeneity of the back-scattered signal^[8-10]. Neoplastic and normal tissue also showed different light backscattering patterns^[11-13].

Subsequent studies were, therefore, performed in *ex vivo* tissue specimens and aimed at comparing OCT imaging with histology, to assess the reliability of the OCT technique to identify and recognize the GI and pancreatico-biliary wall structure. OCT was shown to clearly differentiate the layer structure of the wall^[14].

In vivo studies confirmed the possibility of OCT to recognize the multiple-layer structure of the GI wall^[15,16]; the possibility to introduce the OCT probe into a standard transparent catheter for cannulation during an ERCP procedure permits the epithelial layers of the pancreato-biliary ductal system and sphincter of Oddi to be investigated. From a clinical point of view, OCT imaging of the pancreatic and biliary ductal system could improve the diagnostic accuracy for ductal epithelial changes and the differential diagnosis between neoplastic and non-neoplastic lesions, since in several conditions, X-ray morphology obtained by ERCP and other imaging techniques may be non-diagnostic, and the sensitivity of intraductal brush cytology during ERCP procedures is highly variable.

In our studies, a near-focus OCT probe (Pentax, Lightlab Imaging, Westford, MA, USA) was used, with a penetration depth of about 1 mm and a resolution of approximately 10 μm . The probe operates at 1.2-1.4 μm center wavelength (nominal value: 1.3 μm), with a scan frequency ranging from 1000 to 4000 kHz (nominal value: 3125 kHz). Radial and longitudinal scanning resolutions have an operating range in tissue of 15-20 μm (nominal value: 18 μm), and 21-27 μm (nominal value: 24 μm), respectively. Infrared light is delivered to the imaging site through a single optical fiber 0.006 diameter. OCT probe is assembled in a catheter with an outer

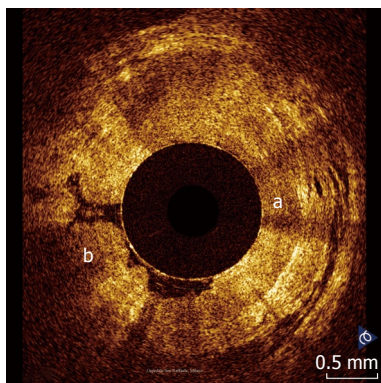


Figure 1 OCT pattern of squamo-columnar junction. The horizontal, layered architecture of the esophageal wall (a) appears clearly distinguishable from the vertical crypt-and-pit architecture of the gastric wall (b).

diameter of 1.2 mm; the catheter-based probe consists of a rotating probe encased in a transparent outer sheath, which remains stationary while the rotating probe has a pullback movement of 1 mm/s, with an acquisition rate of 10 frames per second. Using this technique, a segment of tissue 5.5 cm long can be filmed over a 55-s period.

OCT RECOGNITION OF GI TRACT AND PANCREATICO-BILIARY WALL STRUCTURE IN NORMAL CONDITIONS

GI tract

The esophagus and the esophago-gastric junction has been the most widely investigated organ so far. Esophago-gastric junction appears at OCT investigation clearly recognizable because the stomach wall shows a different OCT pattern, characterized by the presence of a vertical crypt-and-pit architecture of the mucosa that changes abruptly to the horizontal, layered tissue architecture of the esophageal squamous epithelium (Figure 1).

In normal conditions, OCT imaging of esophageal wall recognizes a multiple-layer structure characterized by a superficial weakly scattering (hypo-reflective) layer, corresponding to the squamous epithelium, a highly scattering (hyper-reflective) layer corresponding to the lamina propria, a weakly scattering layer corresponding to the muscularis mucosae, a moderately scattering layer corresponding to the submucosa, and a weakly scattering, deep layer corresponding to muscularis propria (Figure 2). The latter layer is not even recognizable *in vivo*, depending on the depth of penetration of the OCT probe used. Submucosal glands and vessels have also been identified^[5-8]. In a recent *ex vivo* study the muscularis mucosae was distinctly recognized during OCT investigation by using a Ti: Sapphire laser light source^[16].

Overall, the normal esophageal wall architecture shows at OCT imaging a clearly recognizable horizontal, layered structure.

OCT images of the gastric mucosa are characterized by less contrast, depending upon the crypt-and-pit architecture of the glandular epithelium^[2,8,12]. Four

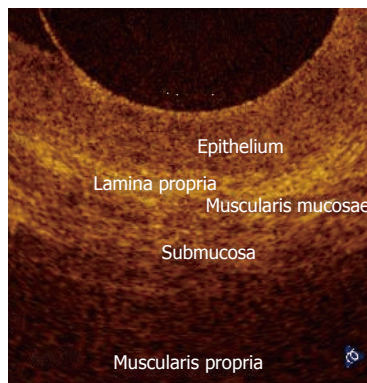


Figure 2 Magnification of a OCT image showing normal esophageal wall. The OCT image shows a multiple-layer structure characterized by a superficial weakly scattering (hypo-reflective) layer, corresponding to the squamous epithelium, a highly scattering (hyper-reflective) layer corresponding to the lamina propria, a weakly scattering layer corresponding to the muscularis mucosae, difficult to recognize, a moderately scattering layer corresponding to the submucosa, and a weakly scattering, deep layer corresponding to muscularis propria.

layers can be identified from the surface: The glandular epithelium, muscularis mucosae, submucosa with blood vessels, and muscularis propria^[9]. Inflammation, as occurs in gastritis, has been reported to produce greater backscattering of the signal and a more pronounced crypt-and-pit pattern architecture, compared with normal tissue^[17].

In the duodenum and small intestine OCT clearly recognizes the mucosa and submucosa with the vascular structure^[5,15]. OCT identified intestinal villous morphology and the degree of atrophy with 100% agreement compared to histology in a study by Hsiung *et al*^[18], who analyzed OCT images *ex vivo* on fresh surgical specimens from the small intestine compared with histology. The ability of OCT imaging to recognize the villous pattern and its alterations could be used to identify celiac disease in real time during standard upper GI endoscopy in patients undergoing endoscopy for conditions often related to a misdiagnosed celiac disease, such iron deficiency anemia, osteoporosis, diabetes mellitus, or autoimmune disorders, and select dyspeptic patients who need biopsies for detecting the disease^[19,20].

In the colon, mucosa and submucosa can also be seen with strong correlation with histology. Mucosa appears as a hyper-reflective layer; submucosa as a hypo-reflective layer with horizontal striations, and the OCT appearance is related to its composition, which could be of assistance in the diagnosis of chronic inflammatory conditions involving the submucosa. Dynamic application of pressure of the OCT probe on the tissue reveals compressibility of both mucosa and submucosa, that may be another criteria for identifying chronic inflammation and fibrosis^[19]. The detection of transmural inflammation serves to distinguish patients with Crohn's disease from those with ulcerative colitis; the detection of dysplasia may help in the follow-up of long-standing chronic inflammatory diseases^[21]. In presence of dysplasia, the detection of lower boundary of the mucosa may help in identifying the extension of dysplastic changes.

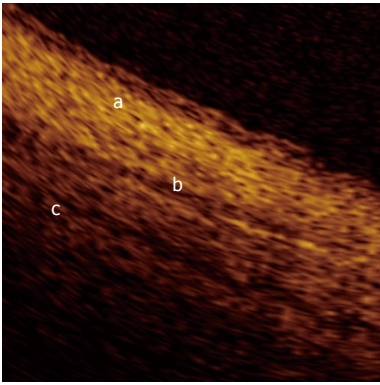


Figure 3 Magnification of an OCT image from the normal common bile duct wall. From the surface of the duct, up to a depth of 1 mm, the following layers are recognizable: the single layer of epithelial cells, approximately 0.04-0.06 mm thick, visible as a superficial, hypo-reflective band (a); the connective-muscular layer surrounding the epithelium, visible as a hyper-reflective layer approximately 0.34-0.48 mm thick (b); the connective layer visible as a hypo-reflective layer with longitudinal relatively hyper-reflective strips (smooth muscle fibers) (c).

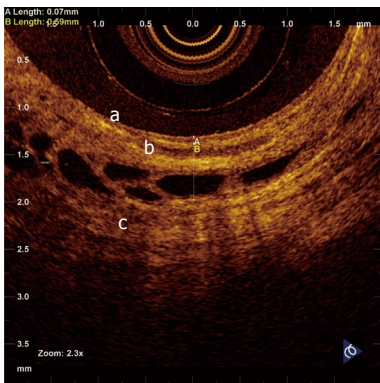


Figure 4 Magnification of an OCT image from the normal sphincter of Oddi wall. From the surface of the duct, up to a depth of 1 mm, the following layers are recognizable: The single layer of epithelial cells, approximately 0.04-0.08 mm thick, visible as a superficial, hypo-reflective band (a); the connective-muscular layer surrounding the epithelium, visible as a hyper-reflective layer approximately 0.23-0.37 mm thick (b); the connective layer visible as a hypo-reflective layer with longitudinal relatively hyper-reflective strips (smooth muscle fibers) (c). Within the intermediate and outer layer vessels are also recognizable, visualized as non-reflecting areas surrounded by a hyper-reflective endothelium. Margins between the intermediate and outer layer are poorly recognizable, due to the irregular distribution of connective and muscular structure.

Pancreatico-biliary ductal system

To date, visualization of the epithelium of the main pancreatic duct has been obtained mainly post-mortem^[22] and *ex vivo* in humans^[23,24], while *in vivo* it comes from one study in animals^[25] and another in humans^[26]. Normal biliary ductal system has been investigated in humans, *ex vivo* in a study^[23] and *in vivo*, in two ERCP-based studies^[27,28]. Sphincter of Oddi structure has also been investigated in normal and pathological conditions either in *ex vivo* or *in vivo* studies^[23,27].

In a recent study by our group^[26], OCT imaging of main pancreatic duct, common bile duct and sphincter of Oddi normal structure has been shown to be able to provide features that were similar to those observed

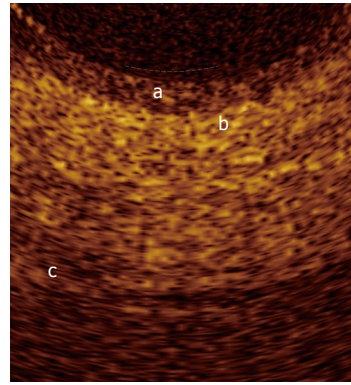


Figure 5 Magnification of an OCT image from the normal main pancreatic duct wall. From the surface of the duct, up to a depth of 1 mm, the following layers are recognizable: The single layer of epithelial cells, approximately 0.04-0.08 mm thick, visible as a superficial, hypo-reflective band (a); the connective-fibro-muscular layer surrounding the epithelium, visible as a hyper-reflective layer approximately 0.36-0.56 mm thick (b); the connective and acinar structure close to the ductal wall epithelium, visible as a hypo-reflective layer (c).

in the corresponding histological specimens in 80% of sections; the agreement between OCT and histology in the definition of normal wall was good (81.8%). OCT images identified three differentiated layers up to a depth of about 1 mm. From the surface of the duct, it was possible to recognize an inner hypo-reflective layer corresponding to the single layer of epithelial cells close to the lumen, an intermediate homogeneous hyper-reflective layer corresponding to the fibro-muscular layer surrounding the epithelium, and an outer, less definite, hypo-reflective layer corresponding to the smooth muscular structure within a connective tissue in the common bile duct and at the level of the sphincter of Oddi, and connective-acinar structure in the main pancreatic duct (Figures 3-5).

The three different layers showed a linear, regular surface and each layer had a homogeneous back-scattered signal in every frame; however, the differentiation between the intermediate and outer layer appeared more difficult than between the inner and intermediate layer. The thickness of the inner and intermediate layers measured by OCT was similar to those measured by histology; the muscular and connective-acinar structure was visible until the working depth of penetration into the tissue of the near-focus probe (about 1 mm).

Smooth muscle structure appeared at OCT scanning as hyper-reflective, longitudinal strips within a context of hypo-reflective tissue and was particularly recognizable at the level of sphincter of Oddi. Veins, arteries and secondary pancreatic ducts were also identifiable by OCT, characterized by hypo- or non-reflective, well delimited areas.

The images acquired in this study provided information on tissue architectural morphology that could have only previously be obtained with conventional biopsy. These results suggest that OCT could become a powerful imaging technology, enabling high-resolution diagnostic images to be obtained from the pancreato-biliary system during a diagnostic ERCP procedure.

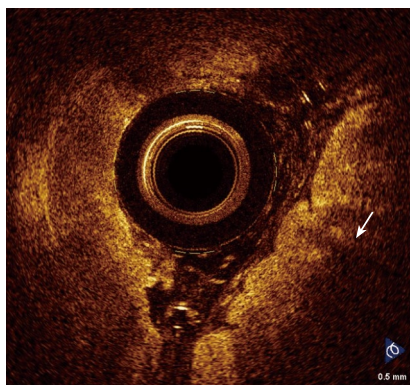


Figure 6 Barrett's esophagus (arrow). OCT features predictive for the presence of intestinal metaplasia are: The absence of the layered structure of the normal squamous epithelium and the presence of the vertical crypt-and-pit morphology of normal gastric mucosa; a disorganized architecture with inhomogeneous backscattering of the signal and an irregular mucosal surface; the presence of submucosal glands characterized by a markedly hypo-reflective tissue below the epithelial surface.

OCT RECOGNITION OF GI TRACT AND PANCREATICO-BILIARY WALL STRUCTURE IN DYSPLASTIC AND NEOPLASTIC CONDITIONS

At present, the exact cause of the disorganized architecture and altered light-scattering associated with dysplastic tissue by OCT imaging is unknown. A number of factors have been suggested, including subcellular morphological changes, altered fibrovascular stroma and abnormal mucin content associated with neoplastic tissue change, proliferation of cells leading to a loss of epithelial and stromal orientation, and altered cytological features such as an increased nuclear-to-cytoplasm ratio that may alter infrared light back-scattering^[9,29].

In its current form and resolution, OCT will likely localize areas displaying architectural distortion to guide biopsy.

GI tract

Most of the so far published studies used OCT imaging to detect dysplasia and early cancer within Barrett's epithelium. Since the penetration depth of OCT does not exceed 1-2 mm, the technique could be useful, not only in detecting dysplasia, but also in staging superficial cancers that are difficult to stage accurately with ultrasound endoscopy. The technique appears, therefore, of crucial importance in the management of the disease.

Barrett's epithelium is characterized by the presence of specialized intestinal metaplasia within the esophageal mucosa. The hallmark histologic feature of specialized intestinal metaplasia is the presence of goblet cells. Identification of Barrett's epithelium is of clinical relevance since the lesion requires endoscopic follow-up, being a recognized precancerous condition. In clinical practice Barrett's epithelium is generally identified by performing multiple biopsies within the areas of gastric metaplasia, either in a random manner or after a

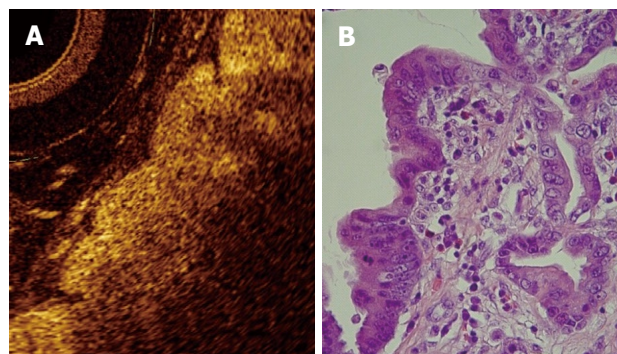


Figure 7 OCT image showing high-grade dysplasia (A) compared to histology (B). Because the degree of reflectivity depends upon nuclear size, a markedly inhomogenous and hypo-reflective back-scattering of the signal should indicate the presence of high-grade dysplasia.

previous vital staining with methylene blue (MB).

Although the inter-subject variability of OCT imaging of normal squamous epithelium and gastric mucosa appears to be low, the OCT imaging of Barrett's epithelium demonstrated a greater variability in the previous published studies. OCT features predictive for the presence of intestinal metaplasia are: (1) the absence of the layered structure of the normal squamous epithelium and the presence of the vertical crypt-and-pit morphology of normal gastric mucosa; (2) a disorganized architecture with inhomogeneous back-scattering of the signal and an irregular mucosal surface; and (3) the presence of submucosal glands characterized at the OCT imaging as pockets of low reflectance below the epithelial surface^[30-32] (Figure 6). When these OCT criteria were applied to images acquired prospectively, the criteria were found to be 97% sensitive and 92% specific for specialized intestinal metaplasia, with a PPV of 84%. The presence of the crypt-and-pit architecture may render difficult to discriminate between intestinal metaplasia and normal or inflamed gastric mucosa^[9].

Unfortunately, up to now, attempts to identify OCT patterns characteristic for dysplasia, mainly the high-grade type, have been substantially disappointing. The increased nuclear-to-cytoplasmic ratio occurring in dysplasia may alter the light reflection characteristics, giving a more inhomogeneous back-scattering of the signal (Figure 7). Because the degree of reflectivity depends upon nuclear size, a markedly homogenous and hypo-reflective back-scattering of the signal should indicate the presence of high-grade dysplasia; moreover, it is possible that by quantitating the OCT signal as a function of depth, OCT would be able to characterize high-grade dysplasia within intestinal metaplasia tissue. Poneros *et al*^[17], by using two parameters of tissue reflectivity as an indicator of dysplasia, retrospectively diagnosed high-grade dysplasia with 100% sensitivity and 85% specificity. Such an accurate analysis of the degree of signal reflectivity requires to avoid areas with incorrect artifact signal properties: This may be obtained by the identification of a precisely defined area with homogeneous signal reflectance, an adequate catheter-tissue contact, and a reduction of motion

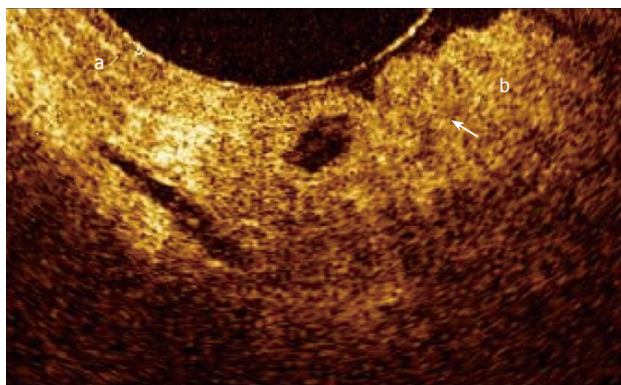


Figure 8 OCT image showing normal oesophageal mucosa (a) and Barrett's epithelium (b) with focal high-grade dysplasia (arrow).

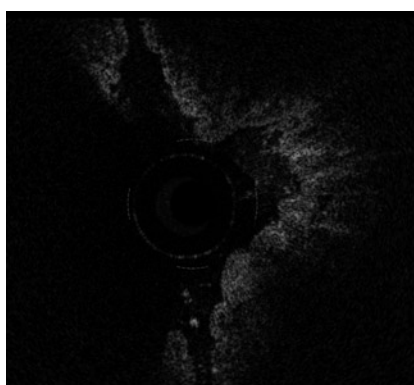


Figure 9 Magnified OCT imaging of early stage adenocarcinoma raised within Barrett's epithelium. The lack of the regular esophageal wall layered morphology and a markedly heterogeneous back-reflectance of the signal characterize the neoplastic lesion, which is confined within the epithelium.

artifacts. More recently, the morphological appearance of the OCT images, rather than the quantitative analysis of the OCT signal in the image, were used for the diagnosis and grading of dysplasia; for this purpose an endoscope fitted with an EMR standard cap was used, to stabilize the mucosal surface and avoid movement from esophageal peristalsis and transmitted cardiac and respiratory motion. In this study sensitivity, specificity, positive predictive value, negative predictive value, and diagnostic accuracy for dysplasia were respectively, 68%, 82%, 53%, 89%, and 78%^[33].

However, with the current available OCT devices, the recognition of dysplasia within intestinal metaplasia and mainly the differentiation between low- and high-grade dysplasia appears difficult^[34] (Figure 8).

OCT features characteristic for adenocarcinoma arising from Barrett's epithelium are the lack of the regular esophageal wall layered morphology and a markedly heterogeneous back-reflectance of the signal^[35,36] (Figure 9). These features permit to clearly identify the lesion and differentiate between the neoplastic and non-neoplastic tissue in advanced disease.

Figure 10 shows and compares OCT findings of normal esophageal mucosa, Barrett's epithelium, dysplasia, and adenocarcinoma.

Despite some studies were conducted about the use

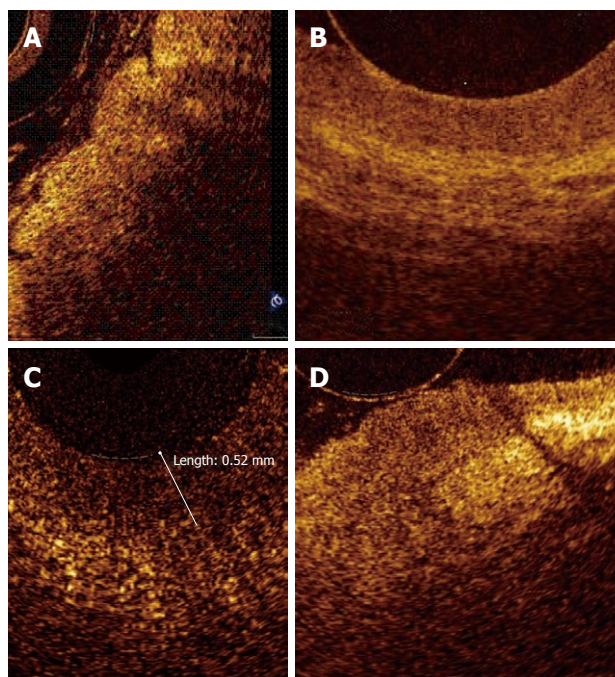


Figure 10 Comparison of OCT findings of normal esophageal mucosa (A), Barrett's epithelium (B), dysplasia (C), and adenocarcinoma (D).

of the OCT in the stomach and small intestine, no data are actually available about its use in detecting dysplasia.

Only few data are present in literature concerning the use of the OCT to detect dysplasia or cancer in the colon^[37-39]. In a study by Pfau *et al.*^[39] on 24 patients, 30 dysplastic adenomas and 14 hyperplastic polyps were studied; the real-time OCT investigation showed that adenomas were more disorganized than the hyperplastic polyps, with a significantly more disorganized structure ($P = 0.0005$). Moreover, the infrared-light back-scattering of the adenomatous polyps appeared more hypo-reflective than hyperplastic ($P = 0.0007$). By using a computer-generated method to quantify the degree of scattering of individual pixels within a specified area in each image (60×60 pixels), it was found that the mean differences in light scattering were significantly greater between adenomatous and normal tissue (mean difference = 45.81), than between hyperplastic polyps and normal tissue (mean difference = 14.86). The real-time OCT infra-red light back-scattering score of polyps was also demonstrated to be a significant predictor of an adenomatous status. However, differently from the dysplasia occurring within Barrett's epithelium, in the study done by these authors defined OCT parameters histologically proven to detect colonic dysplasia were not found.

Pancreatico-biliary ductal system

Pathological pancreatic ductal system has been investigated by our group in humans in two *ex vivo* studies^[14,24] performed on multiple surgical pancreatic specimens obtained from patients with pancreatic head adenocarcinoma.

In chronic inflammatory changes involving the main pancreatic duct, OCT still showed conserved three-layer

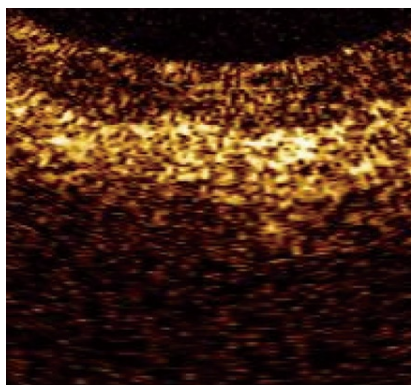


Figure 11 Magnified OCT images from section of main pancreatic duct showing low-grade dysplasia. The surface between the inner and intermediate layers appeared irregular. Dysplasia presents strong hyper-reflectance of the intermediate layer, particularly in the part closest to the inner layer. The outer layer did not differ from other non-malignant conditions and appeared homogeneously hypo-reflective.

architecture. However, the inner, hypo-reflective layer appeared slightly larger than normal and the intermediate layer appeared more hyper-reflective than in normal tissue; this is probably because of the dense mononuclear cell infiltrate. The back-scattered signal was heterogeneous with marked hypo- or hyper-reflectance in some sections. The agreement between OCT and histology in the definition of MPD chronic inflammatory changes was poor (27.7%).

The OCT pattern in presence of dysplasia of the main pancreatic duct epithelium was characterized by an inner layer markedly thickened, strongly hypo-reflective and heterogeneous; this OCT finding is probably due to the initial structural disorganization (increased mitosis and altered nucleus/cytoplasm ratio). The surface between the inner and intermediate layers appeared irregular. As in chronic inflammatory tissue, dysplasia too gave strong hyper-reflectance of the intermediate layer, particularly in the part closest to the inner layer. The outer layer did not differ from other non-malignant conditions and appeared homogeneously hypo-reflective (Figure 11). However, in chronic pancreatitis and dysplasia, only 62% of cases OCT and histology were concordant. The K statistic used to assess agreement between the two procedures was equal to 0.059 for non-neoplastic MPD wall appearance.

Overall, normal wall structure and chronic inflammatory or low-grade dysplastic changes cannot be distinguished in 38% of the sections because the architecture of the layers and surface light reflection did not show a characteristic OCT pattern.

In all sections with histologically proven adenocarcinoma, OCT showed a totally subverted MPD wall architecture. The three layers of the ductal wall and their linear, regular surface, normally giving a homogeneous back-scattered signal, were not recognizable. The margins between the connective-fibro-muscular layer and acinar tissue were unidentifiable. The back-scattering of the signal appeared strongly heterogeneous, with minute, multiple, non-reflective

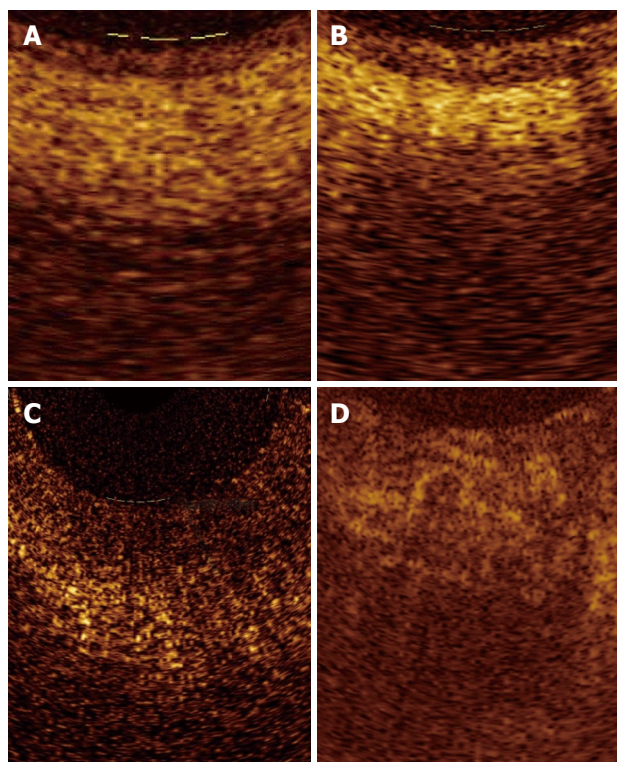


Figure 12 Magnified OCT images from sections with either normal (A), tumor-associated chronic inflammation (B), low-grade dysplasia (C), and adenocarcinoma (D) tissue.

areas in the disorganized pancreatic microstructure. Of sections with adenocarcinoma, OCT and histology were 100% concordant.

Figure 12 shows magnified OCT images from sections of main pancreatic duct with normal tissue, chronic pancreatitis, low-grade dysplasia, and adenocarcinoma.

Totally subverted wall architecture was also observed by OCT in presence of neoplastic tissue within the common bile duct^[40] (Figure 13).

Studies *in vivo* were performed in animals^[25] and humans^[27]. We evaluated the diagnostic accuracy of OCT for the diagnosis of carcinoma, during ERCP, in a series of patients with MPD strictures of unknown etiology. In this study, the accuracy of OCT for detection of neoplastic tissue was 100%, compared with 66.7 % for intraductal brush cytology. The study showed that OCT is feasible during an ERCP procedure and was superior to brush cytology in distinguishing non-neoplastic from neoplastic lesions^[26].

In conclusion, OCT appears a promising technique for real-time, high-resolution, cross-sectional imaging of the inner layer of the wall of the GI and pancreato-biliary tract, during the routine endoscopy. The technique recognizes with high definition the mucosa, muscularis mucosae and submucosa, and seems particularly useful in the study of the esophageal mucosa; given its superior resolution compared with other imaging modalities such as endoscopic ultrasonography (EUS) or catheter-probe EUS (CPEUS), OCT has great potential as a powerful adjunct to standard endoscopy in identification and

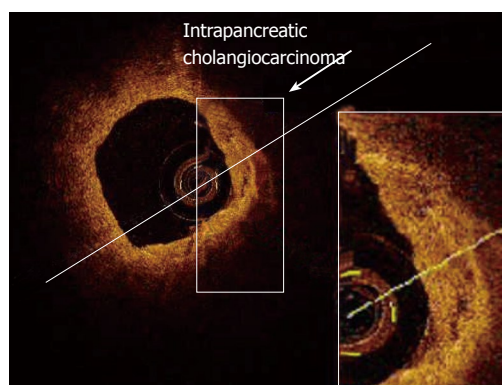


Figure 13 Magnified OCT images of neoplastic tissue within the intrapancreatic portion of the common bile duct.

surveillance of Barrett's epithelium, in order to detect high-grade dysplasia and adenocarcinoma at early stage and identify cases in whom mucosectomy becomes a curative procedure.

In the pancreato-biliary ductal system, OCT can be used to discriminate between non-neoplastic and neoplastic tissue when strictures of unknown etiology are identified during an ERCP procedure, being its diagnostic accuracy higher than reported for intraductal brush cytology.

However, despite the promising studies reported in literature, with the current available OCT devices the recognition of dysplasia within intestinal metaplasia and mainly the differentiation between low- and high-grade dysplasia appears difficult.

On the other hand, since OCT has a penetration depth that does not exceed the 2 mm, it has a greater capability of diagnosing adenocarcinoma confined within mucosa and submucosa and could, therefore, be useful in staging superficial cancers that are difficult to stage accurately by EUS.

Features characteristic for adenocarcinoma within Barrett's epithelium are the lack of the regular layered morphology of the esophageal wall and a markedly heterogeneous back-reflectance of the signal. However, further studies are needed to evaluate whether OCT can identify and stage the lesion at an early stage.

OCT appears more promising in the differential diagnosis between non-neoplastic and neoplastic lesions arising within the pancreato-biliary ductal system, since the ductal wall layered structure can be recognized easier and clearer.

At present, it seems to be fairly premature to affirm that OCT plays a role in the real-time diagnosis of dysplasia *in vivo*. However, improvements in both axial and lateral resolutions to the subcellular level ($< 5 \mu\text{m}$) together with the development of better light sources and optics, may allow dysplastic cells to be better identified in the future. Doppler OCT could also offer a unique ability to provide detailed subsurface imaging of mucosal microvascular networks.

REFERENCES

1 Huang D, Swanson EA, Lin CP, Schuman JS, Stinson WG,

- Chang W, Hee MR, Flotte T, Gregory K, Puliafito CA. Optical coherence tomography. *Science* 1991; **254**: 1178-1181
- 2 Fujimoto JG. Optical coherence tomography for ultra-high resolution *in vivo* imaging. *Nat Biotechnol* 2003; **21**: 1361-1367
- 3 Swanson EA, Huang D, Hee MR, Fujimoto JG, Lin CP, Puliafito CA. High-speed optical coherence domain reflectometry. *Optics Letters* 1992; **17**: 151-153
- 4 Das A, Sivak MV Jr, Chak A, Wong RC, Westphal V, Rollins AM, Willis J, Isenberg G, Izatt JA. High-resolution endoscopic imaging of the GI tract: a comparative study of optical coherence tomography versus high-frequency catheter probe EUS. *Gastrointest Endosc* 2001; **54**: 219-224
- 5 Sivak MV Jr, Kobayashi K, Izatt JA, Rollins AM, Ung-Runyawee R, Chak A, Wong RC, Isenberg GA, Willis J. High-resolution endoscopic imaging of the GI tract using optical coherence tomography. *Gastrointest Endosc* 2000; **51**: 474-479
- 6 Shen B, Zuccaro G Jr. Optical coherence tomography in the gastrointestinal tract. *Gastrointest Endosc Clin N Am* 2004; **14**: 555-571
- 7 Zuccaro G, Gladkova N, Vargo J, Feldchtein F, Zagaynova E, Conwell D, Falk G, Goldblum J, Dumot J, Ponsky J, Gelikonov G, Davros B, Donchenko E, Richter J. Optical coherence tomography of the esophagus and proximal stomach in health and disease. *Am J Gastroenterol* 2001; **96**: 2633-2639
- 8 Bouma BE, Tearney GJ, Compton CC, Nishioka NS. High-resolution imaging of the human esophagus and stomach *in vivo* using optical coherence tomography. *Gastrointest Endosc* 2000; **51**: 467-474
- 9 Poneris JM, Brand S, Bouma BE, Tearney GJ, Compton CC, Nishioka NS. Diagnosis of specialized intestinal metaplasia by optical coherence tomography. *Gastroenterology* 2001; **120**: 7-12
- 10 Tearney GJ, Brezinski ME, Southern JF, Bouma BE, Boppart SA, Fujimoto JG. Optical biopsy in human gastrointestinal tissue using optical coherence tomography. *Am J Gastroenterol* 1997; **92**: 1800-1804
- 11 Pitris C, Jessor C, Boppart SA, Stamper D, Brezinski ME, Fujimoto JG. Feasibility of optical coherence tomography for high-resolution imaging of human gastrointestinal tract malignancies. *J Gastroenterol* 2000; **35**: 87-92
- 12 Kobayashi K, Izatt JA, Kulkarni MD, Willis J, Sivak MV Jr. High-resolution cross-sectional imaging of the gastrointestinal tract using optical coherence tomography: preliminary results. *Gastrointest Endosc* 1998; **47**: 515-523
- 13 Sergeev AM, Gelikonov VM, Gelikonov GV, Feldchtein FI, Kuranov RV, Gladkova ND, Shakhova NM, Snopova LB, Shakhov AV, Kuznetzova LA, Denisenko AN, Pochinko VV, Chumakov YP, Streltsova OS. *In vivo* endoscopic OCT imaging of precancer and cancer states of human mucosa. *Opt Express* 1997; **1**: 432-440
- 14 Testoni PA, Mangiavillano B, Albarello L, Arcidiacono PG, Mariani A, Masci E, Doglioni C. Optical coherence tomography to detect epithelial lesions of the main pancreatic duct: an Ex Vivo study. *Am J Gastroenterol* 2005; **100**: 2777-2783
- 15 Jaekle S, Gladkova N, Feldchtein F, Terentjeva A, Brand B, Gelikonov G, Gelikonov V, Sergeev A, Fritscher-Ravens A, Freund J, Seitz U, Soehendra S, Schroder N. *In vivo* endoscopic optical coherence tomography of the human gastrointestinal tract--toward optical biopsy. *Endoscopy* 2000; **32**: 743-749
- 16 Cilesiz I, Fockens P, Kerindongo R, Faber D, Tytgat G, Ten Kate F, Van Leeuwen T. Comparative optical coherence tomography imaging of human esophagus: how accurate is localization of the muscularis mucosae? *Gastrointest Endosc* 2002; **56**: 852-857
- 17 Poneris JM. Diagnosis of Barrett's esophagus using optical coherence tomography. *Gastrointest Endosc Clin N Am* 2004; **14**: 573-588
- 18 Hsiung PL, Pantanowitz L, Aguirre AD, Chen Y, Phatak D, Ko TH, Bourquin S, Schnitt SJ, Raza S, Connolly JL, Mash-

- mo H, Fujimoto JG. Ultrahigh-resolution and 3-dimensional optical coherence tomography ex vivo imaging of the large and small intestines. *Gastrointest Endosc* 2005; **62**: 561-574
- 19 **Masci E**, Mangiavillano B, Albarello L, Mariani A, Doglioni C, Testoni PA. Optical coherence tomography in the diagnosis of coeliac disease: a preliminary report. *Gut* 2006; **55**: 579
- 20 **Masci E**, Mangiavillano B, Albarello L, Mariani A, Doglioni C, Testoni PA. Pilot study on the correlation of optical coherence tomography with histology in celiac disease and normal subjects. *J Gastroenterol Hepatol* 2007; **22**: 2256-2260
- 21 **Shen B**, Zuccaro G Jr, Gramlich TL, Gladkova N, Trolli P, Kareta M, Delaney CP, Connor JT, Lashner BA, Bevins CL, Feldchtein F, Remzi FH, Bambrick ML, Fazio VW. In vivo colonoscopic optical coherence tomography for transmural inflammation in inflammatory bowel disease. *Clin Gastroenterol Hepatol* 2004; **2**: 1080-1087
- 22 **Tearney GJ**, Brezinski ME, Southern JF, Bouma BE, Boppart SA, Fujimoto JG. Optical biopsy in human pancreatobiliary tissue using optical coherence tomography. *Dig Dis Sci* 1998; **43**: 1193-1199
- 23 **Testoni PA**, Mariani A, Mangiavillano B, Albarello L, Arcidiacono PG, Masci E, Doglioni C. Main pancreatic duct, common bile duct and sphincter of Oddi structure visualized by optical coherence tomography: An ex vivo study compared with histology. *Dig Liver Dis* 2006; **38**: 409-414
- 24 **Testoni PA**, Mangiavillano B, Albarello L, Mariani A, Arcidiacono PG, Masci E, Doglioni C. Optical coherence tomography compared with histology of the main pancreatic duct structure in normal and pathological conditions: an 'ex vivo study'. *Dig Liver Dis* 2006; **38**: 688-695
- 25 **Singh P**, Chak A, Willis JE, Rollins A, Sivak MV Jr. In vivo optical coherence tomography imaging of the pancreatic and biliary ductal system. *Gastrointest Endosc* 2005; **62**: 970-974
- 26 **Testoni PA**, Mariani A, Mangiavillano B, Arcidiacono PG, Di Pietro S, Masci E. Intraductal optical coherence tomography for investigating main pancreatic duct strictures. *Am J Gastroenterol* 2007; **102**: 269-274
- 27 **Poneros JM**, Tearney GJ, Shiskov M, Kelsey PB, Lauwers GY, Nishioka NS, Bouma BE. Optical coherence tomography of the biliary tree during ERCP. *Gastrointest Endosc* 2002; **55**: 84-88
- 28 **Seitz U**, Freund J, Jaekle S, Feldchtein F, Bohnacker S, Thonke F, Gladkova N, Brand B, Schroder S, Soehendra N. First in vivo optical coherence tomography in the human bile duct. *Endoscopy* 2001; **33**: 1018-1021
- 29 **Jaekle S**, Gladkova N, Feldchtein F, Terentjeva A, Brand B, Gelikonov G, Gelikonov V, Sergeev A, Fritscher-Ravens A, Freund J, Seitz U, Schroder S, Soehendra N. In vivo endoscopic optical coherence tomography of esophagitis, Barrett's esophagus, and adenocarcinoma of the esophagus. *Endoscopy* 2000; **32**: 750-755
- 30 **Faruqi SA**, Arantes V, Bhutani MS. Barrett's esophagus: current and future role of endosonography and optical coherence tomography. *Dis Esophagus* 2004; **17**: 118-123
- 31 **Li XD**, Boppart SA, Van Dam J, Mashimo H, Mutinga M, Drexler W, Klein M, Pitris C, Krinsky ML, Brezinski ME, Fujimoto JG. Optical coherence tomography: advanced technology for the endoscopic imaging of Barrett's esophagus. *Endoscopy* 2000; **32**: 921-930
- 32 **Chen Y**, Aguirre AD, Hsiung PL, Desai S, Herz PR, Pedrosa M, Huang Q, Figueiredo M, Huang SW, Koski A, Schmitt JM, Fujimoto JG, Mashimo H. Ultrahigh resolution optical coherence tomography of Barrett's esophagus: preliminary descriptive clinical study correlating images with histology. *Endoscopy* 2007; **39**: 599-605
- 33 **Isenberg G**, Sivak MV Jr, Chak A, Wong RC, Willis JE, Wolf B, Rowland DY, Das A, Rollins A. Accuracy of endoscopic optical coherence tomography in the detection of dysplasia in Barrett's esophagus: a prospective, double-blinded study. *Gastrointest Endosc* 2005; **62**: 825-831
- 34 **Poneros J**. Optical coherence tomography and the detection of dysplasia in Barrett's esophagus. *Gastrointest Endosc* 2005; **62**: 832-833
- 35 **Evans JA**, Nishioka NS. The use of optical coherence tomography in screening and surveillance of Barrett's esophagus. *Clin Gastroenterol Hepatol* 2005; **3**: S8-S11
- 36 **Evans JA**, Poneros JM, Bouma BE, Bressner J, Halpern EF, Shishkov M, Lauwers GY, Mino-Kenudson M, Nishioka NS, Tearney GJ. Optical coherence tomography to identify intramucosal carcinoma and high-grade dysplasia in Barrett's esophagus. *Clin Gastroenterol Hepatol* 2006; **4**: 38-43
- 37 **Anandasabapathy S**. Endoscopic imaging: emerging optical techniques for the detection of colorectal neoplasia. *Curr Opin Gastroenterol* 2008; **24**: 64-69
- 38 **Westphal V**, Rollins AM, Willis J, Sivak MV, Izatt JA. Correlation of endoscopic optical coherence tomography with histology in the lower-GI tract. *Gastrointest Endosc* 2005; **61**: 537-546
- 39 **Pfau PR**, Sivak MV Jr, Chak A, Kinnard M, Wong RC, Isenberg GA, Izatt JA, Rollins A, Westphal V. Criteria for the diagnosis of dysplasia by endoscopic optical coherence tomography. *Gastrointest Endosc* 2003; **58**: 196-202
- 40 **Mangiavillano B**, Mariani A, Petrone MC. An intrapancreatic cholangiocarcinoma detected with optical coherence tomography during endoscopic retrograde cholangiopancreatography. *Clin Gastroenterol Hepatol* 2008; **6**: A30

S- Editor Li DL L- Editor Alpini GD E- Editor Yin DH